Amyloid Self-Assembly

DOI: 10.1002/anie.201408744

Monitoring and Targeting the Initial Dimerization Stage of Amyloid Self-Assembly**

*Yaron Bram, Ayala Lampel, Ronit Shaltiel-Karyo, Anat Ezer, Roni Scherzer-Attali, Daniel Segal, and Ehud Gazit**

Abstract: *Amyloid deposits are pathological hallmark of a large group of human degenerative disorders of unrelated etiologies. While accumulating evidence suggests that early oligomers may account for tissue degeneration, most detection tools do not allow the monitoring of early association events. Here we exploit bimolecular fluorescence complementation analysis to detect and quantify the dimerization of three major amyloidogenic polypeptides; islet amyloid polypeptide, β-amyloid and α-synuclein. The constructed systems provided direct visualization of protein-protein interactions in which only assembled dimers display strong fluorescent signal. Potential inhibitors that interfere with the initial intermolecular interactions of islet amyloid polypeptide were further identified using this system. Moreover, the identified compounds were able to inhibit the aggregation and cytotoxicity of islet amyloid polypeptide, demonstrating the importance of targeting amyloid dimer formation for future drug development.*

The formation of protein amyloid deposits is associated with major human disorders.[1] A partial list of amyloid-associated diseases includes Alzheimer's disease (AD), Parkinson's disease (PD), and Type 2 diabetes (T2D). While tissue degeneration in amyloid disorders is co-localized with the formation of 7–10 nm diameter amyloid fibrils, the nature of the actual cytotoxic agent involved in the pathology of the diseases is still under debate. A typical example is the controversy regarding the role of early soluble oligomers versus mature fibrils of the amyloid beta (Aβ) peptide in the pathology of AD.[2] While in the past most emphasis was directed towards the study of fibrillar assemblies, it is now clear that appearance of the fibrils (leading the formation of amyloid plaques) in the brain merely reflects an end-product in the process of amyloid self-assembly. A key role for smaller, early oligomeric forms of Aβ, and likewise in other amyloidogenic proteins, is now generally accepted in both the cellular toxicity and final pathology of these diseases.[3] Thus, during the last several years substantial efforts focused on the identification, isolation, and characterization of oligomeric forms of various amyloidogenic proteins owing to their probable pathological function as key toxic species. Furthermore, the role of the early oligomers in the process of amyloid fibril assembly remains ambiguous. Several studies have suggested that oligomers represent an obligatory step in the process of fibril formation that is, on-pathway,[4] while other reports suggest that oligomers are formed independently of the pathway to fibril formation, that is, off-pathway.[5] The assembly of both oligomeric and fibrilar conformers is initiated by molecular recognition between structural motifs within the aggregating proteins. The dimerization event is clearly the earliest initial step that precedes any other molecular recognition step. Yet, no monitoring or targeting of this step in readily available. Inhibiting the initial recognition event should prevent the formation of soluble oligomers as well as the assembly of high-molecular-weight fibrilar amyloids.

To specifically study the early dimerization process, we utilized a bimolecular fluorescence complementation assay (BiFC) as an artificial genetic system in *E. coli*, in which the assembled dimer display strong intrinsic fluorescence that allows direct visualization of the protein–protein interaction.[6] The BiFC assay does not require the addition of exogenous fluorogenic or chromogenic agents, avoiding potential non-specific interactions of these agents with the screened compounds in the cells. Moreover, protein-fragment complementation assays (PCAs) that are based on fluorescent proteins are irreversible once assembled.[7] While this property may be unsuitable for kinetic analysis, it can however induce a kinetic trap enabling to capture and visualize amyloidogenic peptide dimers, which are usually highly unstable and transient. Furthermore, this assay was also used to study the oligomerization process of several amyloidogenic peptides including Tau,[8] α-syn,[9] and amyloid β precursor protein (APP).[10]

The BiFC system was constructed using a split mCherry protein.[11] mCherry has a relatively short maturation time and is less affected by fusions to either of its terminal ends compared to the progenitor protein mRFP1.[12] As previously described, mCherry can be divided between residues Asp159 to Gly160 located at a flexible loop outside the β-barrel fold. The 1–159 (NM) and 160–237 (CM) fragments were cloned separately to expression vectors. A flexible linker encoding Gly-Gly-Gly-Gly-Ser ×2 was inserted between the mCherry fragments and their fusion amyloidogenic peptide (Figure 1a). To evaluate the feasibility of the system, we

[*] Dr. Y. Bram, A. Lampel, Dr. R. Shaltiel-Karyo, A. Ezer, Dr. R. Scherzer-Attali, Prof. Dr. D. Segal, Prof. Dr. E. Gazit
Department of Molecular Microbiology and Biotechnology
Tel Aviv 69978 (Israel)
E-mail: ehudg@post.tau.ac.il

[**] This work was supported by the Israel Science Foundation (ISF), 449/11. Furthermore, we would like thank Aviad Levin and Dr. Lihi Adler-Abramovich for their helpful insights and manuscript revisions, Dr. Assaf Shapira for his help with the fluorescent microscopy, Dr. Vered Holdengreber for the help with the transmission electron microscopy and the Gazit and Segal laboratories for productive discussions and comments.

Supporting information for this article is available on the WWW under http://dx.doi.org/10.1002/anie.201408744.

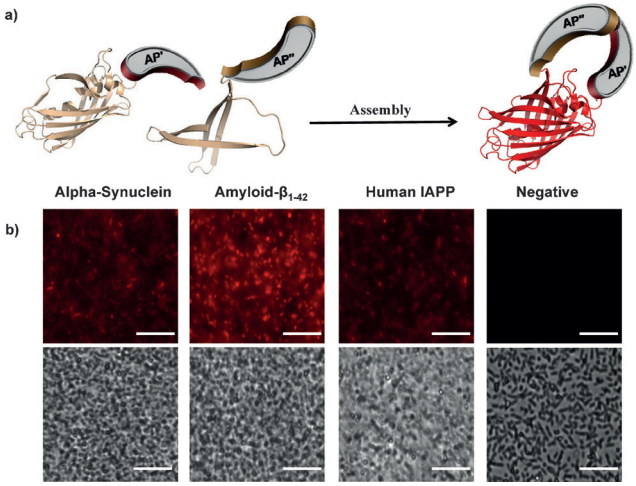

Figure 1. a) Presentation of the BiFC system: split mCHERRY fragments (1–159 (NM), 160–237 (CM)) were fused to the amyloid peptide of interest (AP) in the N′ terminus (AP′) and in the C′ terminus (AP″) using a GGGGSGGGGS linker. b) Fluorescent microscopy of *E. coli* expressing different amyloidogenic peptides, exhibiting a clear red fluorescent signal compared to a negative control expressing the mCherry fragments without fusion counterpart. Scale bars: 20 μM.

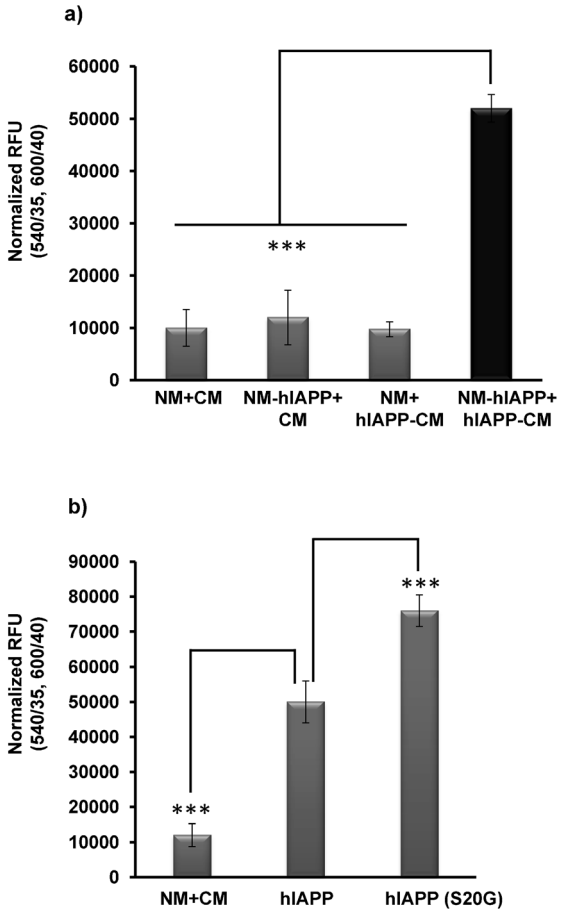

Figure 2. a) BiFC assay of the interaction between split mCHERRY constructs fused to hIAPP. Fluorescence measurements were then taken, with excitation (in nm) 540/35 emission 600/40. A BiFC construct with two copies of hIAPP was compared to the negative controls expressing only one fused IAPP on every fragment or none at all. b) Fluorescence intensity comparison between hIAPP and the missense mutation S20G mutation (hIAPP S20G) that is associated with earlier onset type II diabetes and increased amyloidogenicity and cytotoxicity. Values are means ± s.e.m. ($n = 5$). The statistical significance of differences from wild type were analyzed by Student's t-test (***$P < 0.005$).

examined human islet amyloid polypeptide (hIAPP) associated with T2D, α-synuclein (α-Syn) involved in PD and amyloid-β_{1-42} polypeptide (Aβ) related to AD. Each one of the peptides was expressed along with a negative control (composed of NM and CM fragments without fusion peptides) in *E. coli* and examined (Supporting Information) using fluorescent microscopy. As shown (Figure 1b), the split mCherry fragments, carrying amyloidogenic peptide, constitute an evident red fluorescent signal, while the negative control show no fluorescence. The fluorescence of each of the constructs was also evaluated quantitatively. As shown in Figure 2a, the assay was performed with all of the peptides, all of which exhibited similar trends. (hIAPP-BiFC results are shown as a representative), showing that only the two split mCherry fragments carrying a fusion peptide were able to generate a red fluorescent signal.

To further establish the validity and efficiency of BiFC system, we decided to focus on hIAPP as a model system. We compared the fluorescent signal of serine to glycine missense mutation (S20G) to the wild-type sequence. This mutation was previously reported to be more amyloidogenic and cytotoxic ex vivo and has been associated with genetic tendency for development of T2D at a younger age.[13] The S20G variant produced significantly higher fluorescent signal compared to the native hIAPP peptide, suggesting more assemblies were formed (Figure 2b). This observation indicates that the molecular recognition between the tagged hIAPP monomers in the BiFC system corresponds to the known interaction of the peptide under native physiological conditions. To validate that the fluorescent signal is produced mostly by dimers, lysates of *E. coli* expressing the different BiFC complexes (hIAPP, Aβ, and α-Syn) were analyzed by size-exclusion chromatography (SEC) and the fluorescence intensity of the different fractions was monitored. The fractions with the highest fluorescent signal correlated well with the predicted molecular weight of the dimeric complexes (Figure 3a). Furthermore, the BiFC fluorescent complex migrated as a single band using clear native PAGE (CN-PAGE, Figure 3b). These results suggest that the fluorescent signal derived from dimeric interaction between the amyloidogenic monomers.

To ascertain that the observed interactions depend exclusively on properties of the amyloidogenic peptide, we performed BiFC assembly experiment in vitro. The assembled hIAPP-BiFC complex was purified (Supporting Information), resulting in more than 95% purity. The fluorescent complex was dissociated and denatured by dialysis against buffer with 6M guanidinium chloride (GdmCl). The two hIAPP-BiFC fragments were separated by SEC and examined whether their association can occur in vitro (Figure 3c).

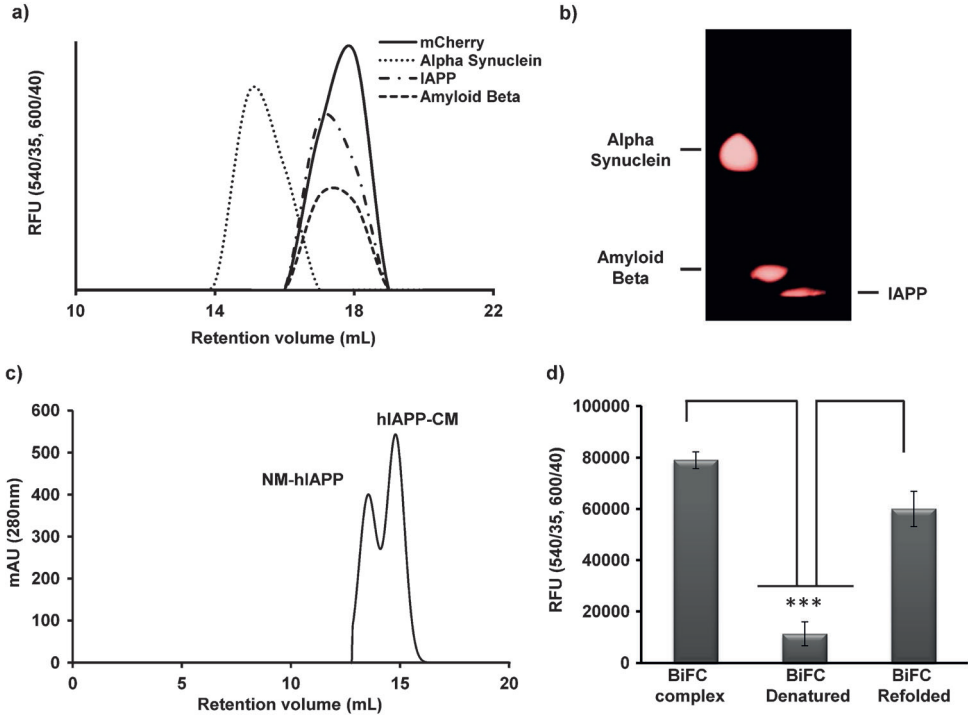

Figure 3. a) Protein lysate extracted from *E.coli* over-expression Aβ, hIAPP, α-Syn BiFC fusions or full-length mCherry were separated by gel filtration chromatography, fluorescence was measured, and size correlation was calculated by a protein standard curve. Fractions with the highest fluorescent signal correlated well to BiFC dimer formation. K_{av} was calculated with the following equation: $y=-0.6411x+3.5074$, $R^2=0.9381$. b) Protein lysate extracted from *E. coli* over-expression Aβ, hIAPP, and α-Syn BiFC fusions were analyzed using CN-PAGE; fluorescence was detected using fluorescence gel imager apparatus (Syngene). c) mCherry complex was purified (see the Supporting Information) and denatured with 6 M GdmCl; the two fragments was separated by gel filtration chromatography. d) Fluorescence comparison of purified mCherry complex: the two fragments of the denatured mCherry complex after separation with gel filtration and combining them together in 1:1 molar concentration and the two fragments of the mCherry complex after refolding together. Following protein refolding, up to 70% of the fluorescence signal was recovered, suggesting that the BiFC association is dependent on the peptide properties and does not mediated by other cellular component. Values are means ± s.e.m. ($n=4$). The statistical significance of differences from wild type were analyzed by Student's t-test (***$P<0.005$).

Following protein refolding, up to about 70% of the fluorescent signal was recovered (Figure 3d), indicating that the BiFC association is not dependent on other cellular components; furthermore, the fluorescent complex formed in vitro exhibited similar SEC retention time, which corresponded to the size of dimeric complex (Supporting Information, Figure S1). Different concentrations of the purified BiFC hIAPP complex were also examined by ThT assay and amyloid fibril formation were not observed for over a week (37 °C), suggesting the mCherry protein provide steric hindrance against the aggregation process (Supporting Information, Figure S2).

Next, we examined the suitability of the BiFC assay as a screening platform for inhibitors of hIAPP dimer formation. First, we analyzed two compounds with known activity towards amyloid aggregation, we chose two quinone–tryptophan compounds (NQTrp and Cl-NQTrp) that we have previously demonstrated to be highly effective aggregation and cytotoxicity inhibitors of several amyloids both in vitro and in vivo.[14] The two compounds effectively inhibited the BiFC complex association, a compound concentration of 100 μM resulted in a decrease of about 60% by NQTrp and about 50% by Cl-NQTrp (Supporting Information, Figure S3). Next, we screened a library of 1280 pharmacologically active compounds (Supporting Information). Each compound was also evaluated on a positive control which included *E. coli* over-expressing the intact mCherry protein, allowing us to exclude compounds affecting protein translation, folding or that has quenching effects. Candidates were also examined in a negative control system; that is, bacteria over-expressing the split mCherry fragments (NM + CM) without hIAPP fusion, allowing us to identify compounds with high autofluorescence. Each compound was tested in triplicates and normalized according to cell quantity. Compounds that reduced the fluorescence by ≥60% and passed the positive and negative selection were considered potential hIAPP assembly inhibitors. Using these criteria, eight compounds were identified (Figure 4a). The positive hits were also examined in the α-Syn BiFC system and did not exhibit a significant reduction of fluorescence, indicating their specificity towards hIAPP interactions (data not shown). Furthermore, all the positive hits had a Z' factor ≥0.4, which is considered appropriate for compound screening (Figure 4b).[15]

We wanted to verify whether the positive compounds identified using the BiFC system inhibit native hIAPP peptide assembly in vitro. To that end, four compounds were examined by thioflavin-T (ThT) binding assay. hIAPP was allowed to form amyloid fibrils either in the absence or in the presence of increasing concentrations of the tested compounds (Figure 5). All tested compounds significantly reduced fibril formation in a dose-dependent manner. A molar ratio of 1:2 in favor of the inhibitors led to a decrease of almost 50% in aggregation. Higher molar ratios (1:5) led to a complete inhibition of fibril formation. The ThT results were confirmed by electron microscopy; the fibrils formed by hIAPP alone were large, broad, and ribbon-like, while the samples containing also the inhibitors showed a marked reduction in amyloid load, and the observed amyloids were significant

a)

Compound name	Fluorescence Reduction (%)
Acetamide	80.9±6.2
Azetidine-2-carboxylic acid	83.1±2.2
5-Aminovaleric acid	80.4±12.6
Tryptamine hydrochloride	72.2±8.6
MNS	64.9±1.5
R(-)-NPA	66.7±3.3
Dipyridamole	61.7±4.9
5-Hydroxy-L-tryptophan	69.9±4.2

b)

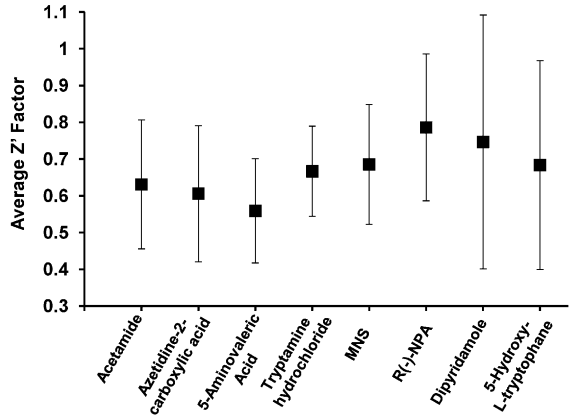

Figure 4. a) Summarization of compounds found by the BiFC screen. The addition of these compounds to the hIAPP-BiFC system resulted in a reduction of the fluorescent signal by over 60% and did not significantly influence the positive and negative control. Values are means ± s.e.m. ($n=3$); the measurements were normalized according to optical density of 700 nm. b) Average Z' factor of the positive compounds found by the BiFC screen. The measurements were normalized according to cell density; values are mean ± s.e.m. ($n=3$).

shorter (Figure 6a). As a negative control, we used two compounds from the chemical library: *O*-(carboxymethyl) hydroxamine hemihydrochloride and protoporphyrin IX. These compounds did not reduce the fluorescent signal of hIAPP BiFC system but had an inhibitory effect on α-syn BiFC complex, which was further confirmed by ThT assay and by TEM analysis (Supporting Information, Figure S4). In correlation with the BiFC results, the two compounds did not show any significant effect on hIAPP aggregation kinetics or on hIAPP amyloid fibrils formation (Supporting Information, Figure S5).

The size distribution of hIAPP assemblies was examined by SEC after two hours of incubation (Supporting Information). As shown in Figure 6b, hIAPP alone eluted in a retention time correspond to high-molecular-weight oligomers, yet the addition of the different compounds to the peptide have shifted the size distribution towards low-molecular-weight population. For example, incubation of hIAPP with 5-hydroxytryptophane elevated the monomeric and dimeric population, tryptamine was shown to be the most effective, shifting almost all of the hIAPP towards a monomeric conformation.

Next, circular dichroism (CD) analysis showed that native hIAPP peptide exhibits a positive peak around 195 nm and a negative peak at 218 nm, indicating a β-sheet conformation. Incubation with the compounds resulted in a reduction of the 218 nm peak amplitude (Figure 6c). The CD analysis along with the SEC and ThT results suggests that the compounds effectively inhibit the aggregation cascade of hIAPP.

To further substantiate the inhibition effect, we tested whether the compounds ameliorate the cytotoxic effect of hIAPP towards pancreatic cells. Upon addition of the hIAPP peptide (10 μM), cell viability decreased by more than 80%. The addition of *O*-(carboxymethyl) hydroxamine hemihydrochloride and protoporphyrin IX correlated with the BiFC and ThT results and did not significantly ameliorate hIAPP cytotoxicity. However, the identified inhibitors reduced sig-

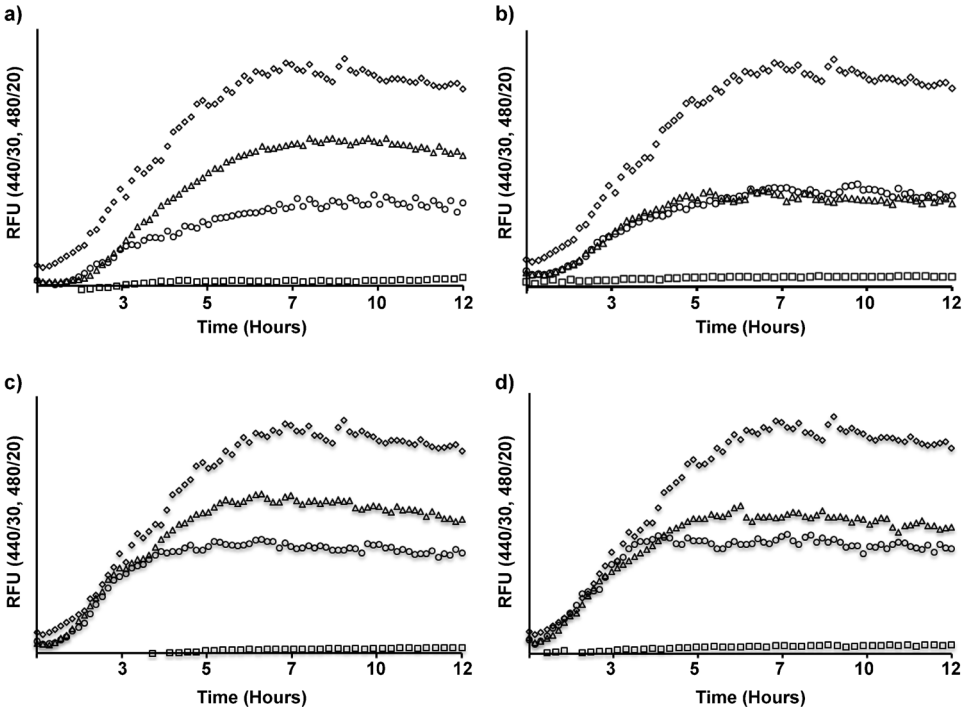

Figure 5. The aggregation of hIAPP quantified in vitro by a ThT binding assay. Kinetic analysis of the inhibition of different compounds towards fibril formation of hIAPP in vitro over the course of 12 h was measured: a) acetamide, b) 5-hydroxy-L-tryptophan, c) tryptamine hydrochloride, d) 5-aminovaleric acid. Each compound was tested with different molar ratios and a good dose-dependent aggregation inhibition was observed. ◇ peptide alone, △ 1:1, ○ 1:2, □ 1:5 molar excess in favor of the compound.

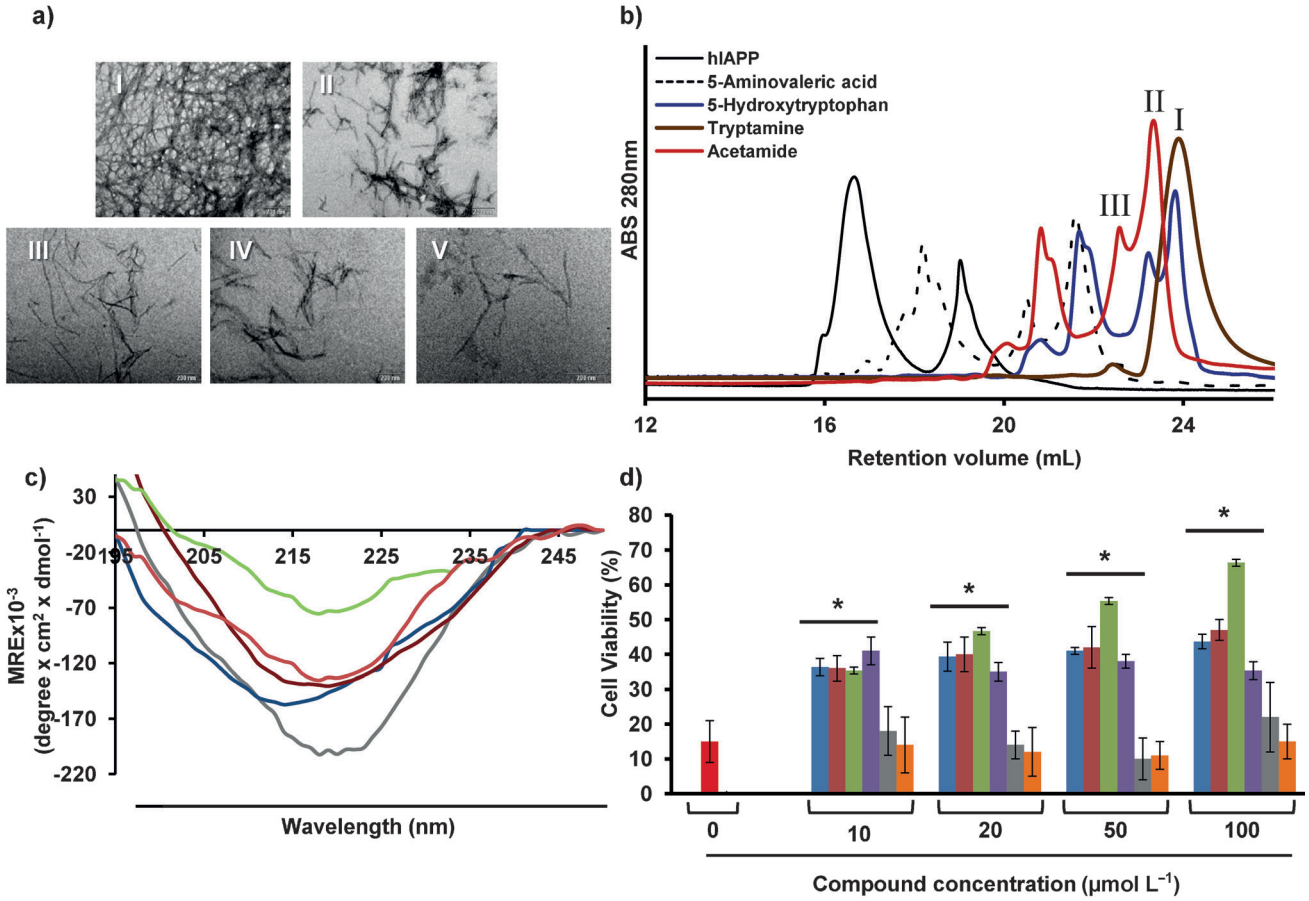

Figure 6. a) Transmission electron microscope (TEM) images taken from the ThT analysis after 12 h. I) peptide alone, II) acetamide, III) 5-hydroxy-L-tryptophan, IV) 5-aminovaleric acid, V) tryptamine hydrochloride. hIAPP/compound molar ratio 1:5, scale bar—200 nm. b) Size-exclusion gel chromatography results of hIAPP co-incubated with the compounds in a 1:5 molar ratio, respectively. I) monomers, II) dimers, III) trimers. c) Circular dichroism spectroscopy of hIAPP alone (gray) or with a 5-fold molar excess of the selected compounds. Acetamide (blue), 5-hydroxy-L-tryptophan (red), 5-sminovaleric acid (scarlet), tryptamine hydrochloride (green); protein concentration 10 µM. Each spectrum represents the average of three measurements. d) Rin-m cells treated with hIAPP (10 µM) with or without the selected compounds in diverse concentration was examined for viability and compared to the non-treated cells. hIAPP alone (red) or with the selected compounds. Acetamide (blue), 5-hydroxy-L-tryptophan (red), 5-sminovaleric acid (purple), tryptamine hydrochloride (green), *O*-(carboxymethyl)hydroxamine hemihydrochloride (gray), protoporphyrin IX (orange). Addition of hIAPP significantly reduced cell viability, while addition of the screened compounds improved significantly the cell viability in a dose-dependent manner ($*P \leq 0.05$).

nificantly the peptide cytotoxicity and dose dependent increase in the viability of the cells was observed (Figure 6). For example, tryptamine was found to be most potent as it increased cell viability up to 60% in a molar ratio of 1:10 in favor of the compound. This analysis is in agreement with the results obtained from the inhibition of hIAPP oligomerization and aggregation in vitro, demonstrating that positive compounds discovered by the BiFC screen are physiologically relevant hIAPP aggregation inhibitors and are able to reduce its toxicity towards pancreatic cells.

In conclusion, we were able to show that the fluorescent signal reflects a genuine protein–protein interaction, which is mostly the result of soluble dimeric species and not from high-molecular-weight aggregates. The screen of pharmacologically active compounds in the BiFC system resulted in several positive hits; the effect of the compounds was further validated in vitro by ThT assay, SEC, and TEM. We further established the inhibition of the selected compounds by demonstrating a dose-dependent decrease in hIAPP cytotoxicity towards pancreatic cells. The correlation between the BiFC screen and the in vitro and ex vivo results demonstrates the significant role of early low-molecular-weight assemblies in the pathological cascade that results in loss of pancreatic β-cell mass.

The assay enables to observe the very first molecular interactions in the assembly process, events that are transient and usually difficult to observe by other complementary methods. Moreover, the scientific community has long debated the actual toxic assembly in different amyloid associated diseases, and various reports point towards different oligomeric assemblies as the actual toxic species. Targeting the very first intermolecular interactions eliminates the problematic search for isolating and identifying the true toxic conformers for clinical purposes, as dimeric interactions are obligatory step in the formation of all the different assemblies. Furthermore, the screen can be fully automated, thus fulfilling

the necessary requirements for a successful high-throughput system.

Received: September 3, 2014
Revised: November 3, 2014
Published online: December 22, 2014

Keywords: amyloid inhibitors · amyloid self-assembly · complementation assays · fluorescence · self-assembly

[1] a) F. Chiti, C. M. Dobson, *Annu. Rev. Biochem.* **2006**, *75*, 333; b) D. Eisenberg, M. Jucker, *Cell* **2012**, *148*, 1188.
[2] J. Hardy, D. J. Selkoe, *Science* **2002**, *297*, 353.
[3] M. E. Larson, S. E. Lesne, *J. Neurochem.* **2012**, *120*, 125.
[4] a) J. D. Harper, S. S. Wong, C. M. Lieber, P. T. Lansbury, Jr., *Biochemistry* **1999**, *38*, 8972; b) T. R. Serio, A. G. Cashikar, A. S. Kowal, G. J. Sawicki, J. J. Moslehi, L. Serpell, M. F. Arnsdorf, S. L. Lindquist, *Science* **2000**, *289*, 1317.
[5] a) A. Kumar, L. C. Paslay, D. Lyons, S. E. Morgan, J. J. Correia, V. Rangachari, *J. Biol. Chem.* **2012**, *287*, 21253; b) G. P. Gellermann, H. Byrnes, A. Striebinger, K. Ullrich, R. Mueller, H. Hillen, S. Barghorn, *Neurobiol. Dis.* **2008**, *30*, 212.
[6] T. K. Kerppola, *Nat. Rev. Mol. Cell Biol.* **2006**, *7*, 449.
[7] a) C.-D. Hu, Y. Chinenov, T. K. Kerppola, *Mol. Cell* **2002**, *9*, 789; b) T. J. Magliery, C. G. M. Wilson, W. Pan, D. Mishler, I. Ghosh, A. D. Hamilton, L. Regan, *J. Am. Chem. Soc.* **2005**, *127*, 146; c) B. Nyfeler, S. W. Michnick, H.-P. Hauri, *Proc. Natl. Acad. Sci. USA* **2005**, *102*, 6350.
[8] W. Chun, G. S. Waldo, G. V. Johnson, *J. Neurochem.* **2007**, *103*, 2529.
[9] T. F. Outeiro, P. Putcha, J. E. Tetzlaff, R. Spoelgen, M. Koker, F. Carvalho, B. T. Hyman, P. J. McLean, *PLoS One* **2008**, *3*, e1867.
[10] C. D. Chen, S. Y. Oh, J. D. Hinman, C. R. Abraham, *J. Neurochem.* **2006**, *97*, 30.
[11] J.-Y. Fan, Z.-Q. Cui, H.-P. Wei, Z.-P. Zhang, Y.-F. Zhou, Y.-P. Wang, X.-E. Zhang, *Biochem. Biophys. Res. Commun.* **2008**, *367*, 47.
[12] N. C. Shaner, R. E. Campbell, P. A. Steinbach, B. N. Giepmans, A. E. Palmer, R. Y. Tsien, *Nat. Biotechnol.* **2004**, *22*, 1567.
[13] a) Z. Ma, G. T. Westermark, S. Sakagashira, T. Sanke, Å. Gustavsson, H. Sakamoto, U. Engström, K. Nanjo, P. Westermark, *Amyloid* **2001**, *8*, 242; b) P. Cao, L.-H. Tu, A. Abedini, O. Levsh, R. Akter, V. Patsalo, A. M. Schmidt, D. P. Raleigh, *J. Mol. Biol.* **2012**, *421*, 282.
[14] a) R. Scherzer-Attali, R. Pellarin, M. Convertino, A. Frydman-Marom, N. Egoz-Matia, S. Peled, M. Levy-Sakin, D. E. Shalev, A. Caflisch, E. Gazit, *PLoS One* **2010**, *5*, e11101; b) R. Scherzer-Attali, D. Farfara, I. Cooper, A. Levin, T. Ben-Romano, D. Trudler, M. Vientrov, R. Shaltiel-Karyo, D. Shalev, N. Segev-Amzaleg, *Neurobiol. Dis.* **2012**, *46*, 663; c) R. Scherzer-Attali, R. Shaltiel-Karyo, Y. H. Adalist, D. Segal, E. Gazit, *Proteins Struct. Funct. Bioinf.* **2012**, *80*, 1962.
[15] a) J.-H. Zhang, T. D. Chung, K. R. Oldenburg, *J. Biomol. Screening* **1999**, *4*, 67; b) J. Hughes, S. Rees, S. Kalindjian, K. Philpott, *Br. J. Pharmacol.* **2011**, *162*, 1239.

